Electromagnetic excitation of nuclei and neutron evaporation in ultrarelativistic ultraperipheral heavy ion collisions

Mariola Kłusek-Gawenda,[1,*] Michał Ciemała,[1,†] Wolfgang Schäfer,[1,‡] and Antoni Szczurek[1,2,§]
[1]*Institute of Nuclear Physics PAN, PL-31-342 Cracow, Poland*
[2]*University of Rzeszów, PL-35-959 Rzeszów, Poland*
(Received 15 November 2013; revised manuscript received 21 March 2014; published 16 May 2014)

We present a new approach for calculating the electromagnetic excitation of nuclei as well as probabilities of emission and different distributions of neutrons from decays of excited nuclear systems for ultrarelativistic, ultraperipheral heavy ion collisions. Excitation functions for $\gamma + \mathrm{Pb} \to \mathrm{Pb}^*$ and $\gamma + \mathrm{Au} \to \mathrm{Au}^*$ are parametrized using physics-motivated components: the excitation of giant resonances, quasideuteron absorption mechanism, excitation of nucleon resonances, as well as high-energy dissociation of protons and neutrons. Neutron emission (up to ten neutrons) from low-energy excitations of ^{208}Pb and ^{197}Au is modeled in terms of the Hauser-Feshbach formalism. The probabilities of a given number of neutrons are calculated as a function of excitation energy in a Monte Carlo code GEMINI++. These probabilities are parametrized by smooth analytical functions. The results are compared to appropriate data for the γ Pb $\to$ Pb* $\to kn$ and γ Au $\to$ Au* $\to kn$ reaction. As an example, the approach is used for calculating electromagnetic excitation in ultraperipheral heavy ion collisions (UPC) processes. Both single-photon and double-photon excitations are included and discussed. Topological cross sections with a given number of neutrons in the forward and backward directions are calculated at the Relativistic Heavy Ion Collider (RHIC) and Large Hadron Collider (LHC) energies. Excitation functions are presented. The results of the calculation are compared to Super Proton Synchrotron (SPS), RHIC, and more recent A Large Ion Collider Experiment (ALICE) experimental data and good agreement is achieved.

DOI: 10.1103/PhysRevC.89.054907 PACS number(s): 25.75.−q, 25.20.−x

I. INTRODUCTION

The exclusive production of mesons, pairs of quark and antiquark particles, pairs of leptons, or other standard model particles in ultraperipheral heavy ion collisions (UPC) has been attracting much attention recently [1,2]. A measurement of such reactions at the high energies of present day colliders [Relatavistic Heavy Ion Collider (RHIC), Large Hadron Collider (LHC)] often requires special triggers. Large charges of colliding ions lead to the production of huge fluxes of associated photons. These photons when scattered on the collision partner can lead to its excitation. As will be discussed in the present paper, low-energy excitations ($E^* < 50$ MeV) play an especially important role. The low-energy excited nuclear heavy systems, close to the giant resonance region, decay predominantly via the emission of a few neutrons. Because the energy of the emitted neutrons in the nucleus rest frame is rather small (∼10–20 MeV), in UPCs the neutrons are emitted in very small cones around beam directions. Such neutrons can be registered by the so-called zero-degree calorimeters (ZDC's), which are associated with many high-energy detectors, such as, e.g., the Solenoidal Tracker (STAR) at RHIC [3] and A Large Ion Collider Experiment (ALICE) at LHC [4].

In the present paper we wish to present our approach, which includes description of the photoexcitation of nuclei and the decay of excited nuclei in the framework of the Hauser-Feshbach theory. The results of our calculations for γ Au $\to$ Au* kn and γ Pb $\to$ Pb* kn are confronted with existing experimental data. Then topological cross sections with a given number of neutrons in ion-ion collisions are calculated and compared to RHIC and LHC data. We discuss the role of single-photon and double-photon excitations. We present simple parametrizations of the relevant impact parameter profiles, which can be conveniently used for a multitude of central final states produced in diffractive or $\gamma\gamma$ subprocesses, such as vector mesons, leptons, pions, and so on.

II. FORMALISM

A. Electromagnetic excitation in UPC

In this section we collect the classical probability calculus methods needed [5–7] to describe the electromagnetic excitation of ions in UPCs due to multiple photon exchanges.

From the usual Weizsäcker-Williams flux of photons $N_A(E,\mathbf{b})$ and the total photoabsorption cross section $\sigma_{\mathrm{tot}}(\gamma A; E)$ discussed in Sec. III, we introduce the mean number of photons absorbed by a nucleus A_2 in the collision with nucleus A_1:

$$\bar{n}_{A_2}(\mathbf{b}) \equiv \int_{E_{\mathrm{min}}}^{\infty} dE\, N_{A_1}(E,\mathbf{b})\sigma_{\mathrm{tot}}(\gamma A_2; E)\,. \tag{2.1}$$

Here the upper limit in the integral is only formal: the photon flux (see any of the reviews in Ref. [1])

$$N_A(E,\mathbf{b}) = \frac{1}{E}\,\frac{Z^2\alpha_{\mathrm{em}}}{\pi^2}\,\frac{1}{\mathbf{b}^2}\,\xi^2 K_1^2(\xi), \quad \xi = \frac{Eb}{\gamma_{\mathrm{lab}}}, \tag{2.2}$$

*mariola.klusek@ifj.edu.pl
†michal.ciemala@ifj.edu.pl
‡wolfgang.schafer@ifj.edu.pl
§antoni.szczurek@ifj.edu.pl

implicitly contains a cutoff in energy. Above E is the photon energy in the rest frame of nucleus A_2, Z is the nuclear charge, and K_1 is a modified Bessel function. The boost to the rest frame of nucleus A_2 is given by

$$\gamma_{\rm lab} = 2\gamma_{\rm cm}^2 - 1\,, \quad \gamma_{\rm cm} = \frac{\sqrt{s_{NN}}}{2m_N}\,. \tag{2.3}$$

The lower limit of integration $E_{\rm min}$ is the threshold for photoexcitation. For statistically independent absorption, we can state the probability of absorption of n photons at impact parameter $\mathbf{b}$ in the Poissonian form

$$w_n(\mathbf{b}) = \frac{(\bar{n}_A(\mathbf{b}))^n}{n!}\,\exp[-\bar{n}_A(\mathbf{b})]\,. \tag{2.4}$$

We define the probability density for a single photon to excite nucleus A_2 in a collision at impact parameter $\mathbf{b}$ of the A_1-A_2 collision as

$$p_{A_2}^{(1)}(E,\mathbf{b}) = \frac{N_{A_1}(E,\mathbf{b})\sigma_{\rm tot}(\gamma A_2;E)}{\bar{n}_{A_2}(\mathbf{b})}\,, \tag{2.5}$$

which is fulfilled, at each $\mathbf{b}$

$$\int_{E_{\rm min}}^{\infty} dE\; p_{A_2}^{(1)}(E,\mathbf{b}) = 1\,. \tag{2.6}$$

Still under the assumption of statistical independence, n photons will excite the nucleus with the probability density

$$p_{A_2}^{(n)}(E,\mathbf{b}) = \int dE_1 dE_2,\ldots,dE_n\,\delta\left(E - \sum_{j=1}^{n} E_j\right) \times p_{A_2}^{(1)}(E_1,\mathbf{b}) p_{A_2}^{(1)}(E_2,\mathbf{b}),\ldots,p_{A_2}^{(1)}(E_n,\mathbf{b}). \tag{2.7}$$

All the n-photon probability densities are properly normalized as follows:

$$\int_{E_{\rm min}}^{\infty} dE\; p_{A_2}^{(n)}(E,\mathbf{b}) = 1\,. \tag{2.8}$$

Below we will explicitly calculate processes up to $n = 2$ photon exchanges, see the diagrams in Figs. 1 and 2.

Then the probability for the excitation of nucleus A_2 in the n-photon process is given by

$$w_n(\mathbf{b}) p_{A_2}^{(n)}(E,\mathbf{b})\,. \tag{2.9}$$

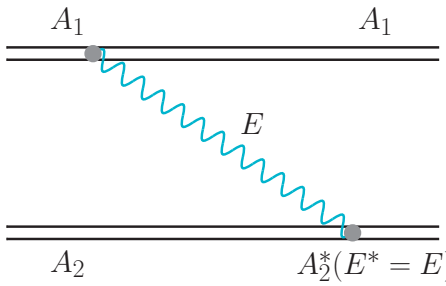

FIG. 1. (Color online) Single excitation in UPCs.

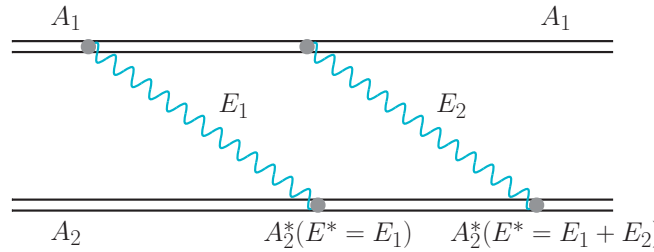

FIG. 2. (Color online) Double excitation in UPCs.

We should sum over all numbers of photons

$$\frac{dP_{A_2}^{\rm exc}(\mathbf{b})}{dE} = \sum_n w_n(\mathbf{b}) p_{A_2}^{(n)}(E,\mathbf{b}) \approx \exp\left[-\bar{n}_{A_2}(\mathbf{b})\right] N_{A_1}(E,\mathbf{b})\sigma_{\rm tot}(\gamma A_2;E), \tag{2.10}$$

where we indicate that we expect the single-photon absorption to dominate. Notice that this may, in practice, depend on the impact parameter. The total probability for the nucleus to be excited is then

$$P_{A_2}^{\rm exc}(\mathbf{b}) = \int dE \frac{dP_{A_2}^{\rm exc}(\mathbf{b})}{dE} = 1 - \exp[-\bar{n}_{A_2}(\mathbf{b})] = \exp\left[-\bar{n}_{A_2}(\mathbf{b})\right]\left(\exp\left[\bar{n}_{A_2}(\mathbf{b})\right] - 1\right) \approx \bar{n}_{A_2}(\mathbf{b})\exp\left[-\bar{n}_{A_2}(\mathbf{b})\right]. \tag{2.11}$$

The excitation cross section is then

$$\sigma_{\rm tot}(A_1A_2 \to A_1A_2^*) = \int d^2\mathbf{b}\; P_{\rm surv}(\mathbf{b}) P_{A_2}^{\rm exc}(\mathbf{b}) = \int d^2\mathbf{b} P_{\rm surv}(\mathbf{b})\left(1 - \exp\left[-\bar{n}_{A_2}(\mathbf{b})\right]\right)\,. \tag{2.12}$$

Sometimes we are interested in the excitation cross section containing only excitations up to $E_{\rm max} \lesssim 100\,$MeV, then we can calculate the cross section from

$$\sigma_{\rm tot}(A_1A_2 \to A_1A_2^*;E_{\rm max}) \approx \int d^2\mathbf{b} P_{\rm surv}(\mathbf{b})\exp[-\bar{n}_{A_2}(\mathbf{b})] \times \int_{E_{\rm min}}^{E_{\rm max}} dE\, N_{A_1}(E,\mathbf{b})\sigma_{\rm tot}(\gamma A_2;E)\,. \tag{2.13}$$

Here

$$P_{\rm surv}(\mathbf{b}) \sim \theta(|\mathbf{b}| - (R_{A_1} + R_{A_2})) \tag{2.14}$$

is the probability for the nuclei to survive the collision without additional strong interactions. As is apparent,

$$w_0(\mathbf{b}) = \exp[-\bar{n}_{A_2}(\mathbf{b})] \tag{2.15}$$

is the contribution to the survival probability from the electromagnetic dissociation channels. The cross section for mutual electromagnetic dissociation can be obtained from

$$\sigma_{\rm tot}(A_1A_2 \to A_1^*A_2^*) = \int d^2\mathbf{b}\; P_{\rm surv}(\mathbf{b}) P_{A_2}^{\rm exc}(\mathbf{b}) P_{A_1}^{\rm exc}(\mathbf{b})\,. \tag{2.16}$$

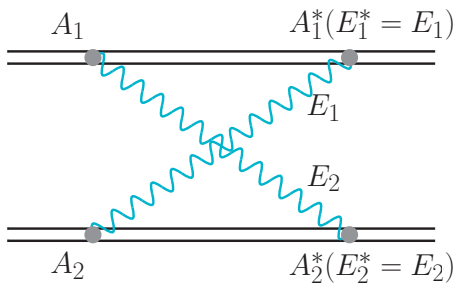

FIG. 3. (Color online) Minimal mechanism for mutual excitation in UPCs.

In Fig. 2 we show the situation when two photons emitted by one of the colliding nuclei hit the second nucleus. Finally, in Fig. 3 we show as an example the case when each of the nuclei emit a photon that then excites the collision partner. We shall call this case mutual excitations. The diagram shows the minimal mechanism needed to excite both nuclei simultaneously. Higher-order diagrams are possible as well.

B. Dissociation into specific final states

In the present paper we are interested mainly in final states that contain a few neutrons and want to study excitation cross sections as a function of neutron multiplicity (a type of "topological cross section"). Here the crucial input are the fractions $f(E,k)$ of a final state with k neutrons coming from the decay of an excited nucleus at excitation energy E. With their help, we can calculate the impact parameter profiles for processes with k evaporated neutrons as

$$\frac{dP^{\rm exc}_{A_2}(\mathbf{b},k)}{dE} = f(E,k)\cdot\sum_n w_n(\mathbf{b}) p^{(n)}_{A_2}(E,\mathbf{b}) \approx f(E,k)\, p^{(1)}_{A_2}(E,\mathbf{b})\bar{n}_{A_2}(\mathbf{b})\exp[-\bar{n}_{A_2}(\mathbf{b})], \tag{2.17}$$

and, correspondingly,

$$P^{\rm exc}_{A_2}(\mathbf{b},k) = \int_{E_{\rm min}}^{E_{\rm max}} dE \frac{dP^{\rm exc}_{A_2}(\mathbf{b},k)}{dE}\,. \tag{2.18}$$

In Fig. 4 we plot these distributions as a function of the impact parameter for $k = 1,2,3$ at $\gamma_{\rm c.m.} = 1470$. The cross section for k-neutron excitation is then

$$\sigma(A_1A_2 \to A_1(k{\rm N},X)) = \int d^2\mathbf{b}\, P_{\rm surv}(\mathbf{b})\, P^{\rm exc}_{A_2}(\mathbf{b},k). \tag{2.19}$$

Of course, we are confined to low-neutron multiplicities, as final states of a large number of the neutron (k) can be produced by processes in the energy region $E > E_{\rm max}$, which we do not model so far. Analogously, the mutual excitation cross sections with m and k neutrons in the debris of nucleus A_1, A_2, respectively, are

$$\sigma(A_1A_2 \to (m{\rm N},X)(k{\rm N},Y)) = \int d^2\mathbf{b}\, P_{\rm surv}(\mathbf{b})\, P^{\rm exc}_{A_1}(\mathbf{b},m)\, P^{\rm exc}_{A_2}(\mathbf{b},k)\,. \tag{2.20}$$

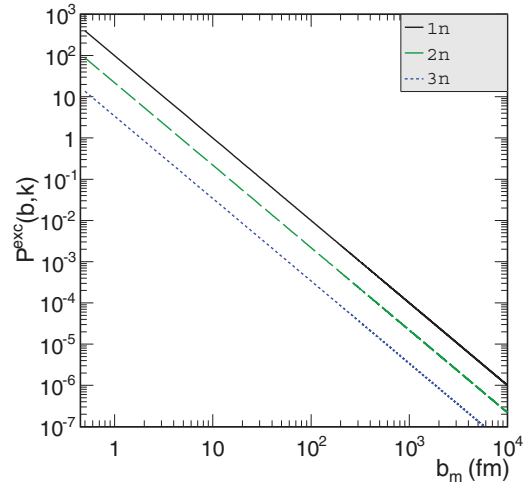

FIG. 4. (Color online) Impact parameter profile for processes with evaporation of $k = 1,2,3$ neutrons from lead nuclei.

III. PHOTON-INDUCED EXCITATION OF NUCLEI AND NEUTRON EVAPORATION

To evaluate the photoabsorption probabilities, we need a parametrization of the total photoabsorption cross section over a broad range of energies. Here we are not interested in a microscopic modeling of the different mechanisms that play an important role at different energies, but rather in a fit of empirical data. At the lowest energies of relevance, photoabsorption is dominated by the giant resonances.

The energy dependence of the cross section for the giant dipole resonance (GDR) component ($\sigma_{\rm GDR}$) is parametrized following Refs. [8,9]:

$$\sigma_{\rm GDR} = \frac{2}{\pi}\sigma_{TRK}\frac{E^2\Gamma_r}{\left(E^2 - E_r^2\right)^2 + (E\Gamma_r)^2} S_r\,. \tag{3.1}$$

The parameters $\sigma_{TRK} = 60\frac{NZ}{A}$ mb MeV, $E_r^{\rm Au} = 13.712$ MeV, $\Gamma_r^{\rm Au} = 4.517$ MeV, $S_r^{\rm Au} = 1.35416$, $E_r^{\rm Pb} = 13.373$ MeV, $\Gamma_r^{\rm Pb} = 3.938$ MeV, and $S_r^{\rm Pb} = 1.33716$ for Au are taken from Ref. [10] and for Pb from Ref. [11].

At somewhat larger energies a so-called quasideuteron contribution plays an important role and following the authors of Ref. [12] is parametrized as

$$\sigma_{\rm QD} = 6.5\frac{NZ}{A}\sigma_d f(E)\,, \tag{3.2}$$

where

$$\sigma_d = 61.2\frac{(E-2.224)^{3/2}}{E^3}\ {\rm mb}\,, \tag{3.3}$$

$$f(E < 20\,{\rm MeV}) = \exp(-73.3/E),$$
$$f(20 < E < 140\,{\rm MeV}) = 8.3714\times10^{-2} - 9.8343\times10^{-3}E + 4.1222\times10^{-4}E^2 - 3.4762\times10^{-6}E^3 + 9.3537\times10^{-9}E^4\,,$$
$$f(E > 140\,{\rm MeV}) = \exp(-24.2/E)\,. \tag{3.4}$$

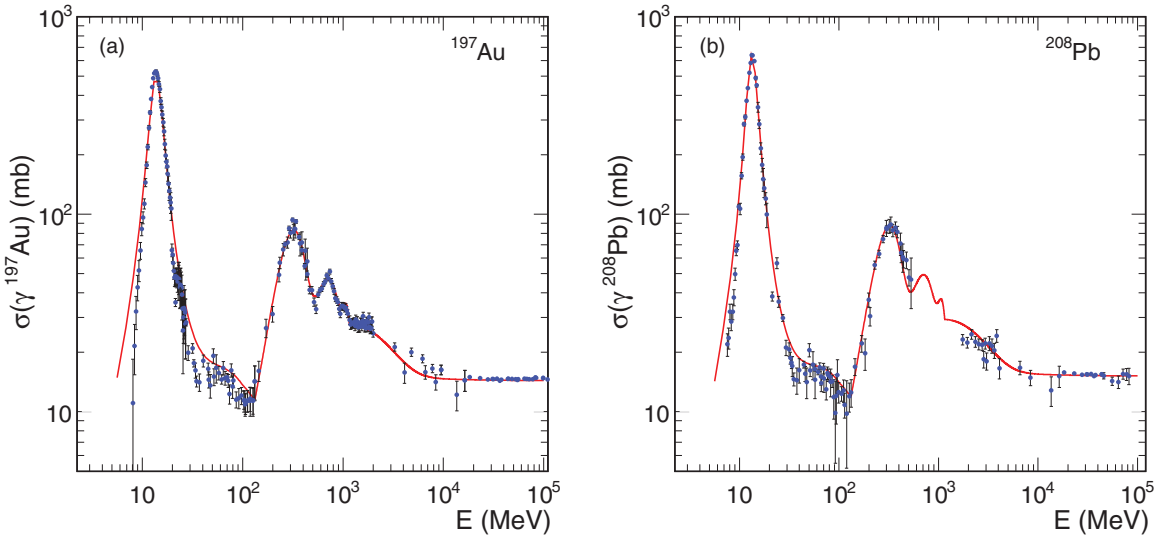

FIG. 5. (Color online) Photoabsorption cross section for the $\gamma\,^{197}\mathrm{Au} \rightarrow {}^{197}\mathrm{Au}$ (left panel) and for the $\gamma\,^{208}\mathrm{Pb} \rightarrow {}^{208}\mathrm{Pb}$ reaction (right panel).

Above a photon energy $E_\gamma > 100$ MeV the nucleon resonances are taken into account, with the Δ resonance being the dominant feature of the excitation spectrum. We parametrize this region of the photoabsorption cross section as a sum of three ($i = 1,2,3$) Gaussian functions

$$\sigma^i_{\mathrm{Gauss}} = \exp\left(\frac{-\left(E-\mu^i_G\right)^2}{2\left(\sigma^i_G\right)^2}\right), \tag{3.5}$$

where $C^1_G = 17$ barn MeV, $\sigma^1_G = 90$ MeV, $\mu^1_G = 315$ MeV, $C^2_G = 19$ barn MeV, $\sigma^2_G = 200$ MeV, $\mu^2_G = 700$ MeV, $C^3_G = 4$ barn MeV, $\sigma^3_G = 90$ MeV, and $\mu^3_G = 1.09$ GeV. The above parameters are for Pb. For the Au nucleus, the Gaussian function is scaled by 197/208.

Above $E_\gamma > 0.5$ GeV the resonant contributions disappear and the continuum related to the breakup of nucleons starts to be important.

For energies between 1 and 8 GeV we describe the data by using an exponential function

$$\sigma_{\mathrm{exp}} = C_{\mathrm{exp}}(E-\mu_{\mathrm{exp}})\exp\left(\frac{-(E-\mu_{\mathrm{exp}})}{\sigma_{\mathrm{exp}}}\right), \tag{3.6}$$

where the parameters are $C_{\mathrm{exp}} = 0.032$ mb/MeV, $\sigma_{\mathrm{exp}} = 1.05$ GeV, and $\mu_{\mathrm{exp}} = 100$ MeV.

For the high-energy part ($E_\gamma > 8$ GeV) we use a simple form given in Ref. [13]

$$\sigma_{\gamma Pb} = \left(15.2 + 0.06\ln^2\left(\frac{E}{\omega_0}\right)\right)\ \mathrm{mb}. \tag{3.7}$$

For the nucleus ^{197}Au, this is scaled by 197/208. This multicomponent parametrization is compared to the experimental data for photoabsorption on Au and Pb [14] in Fig. 5. The

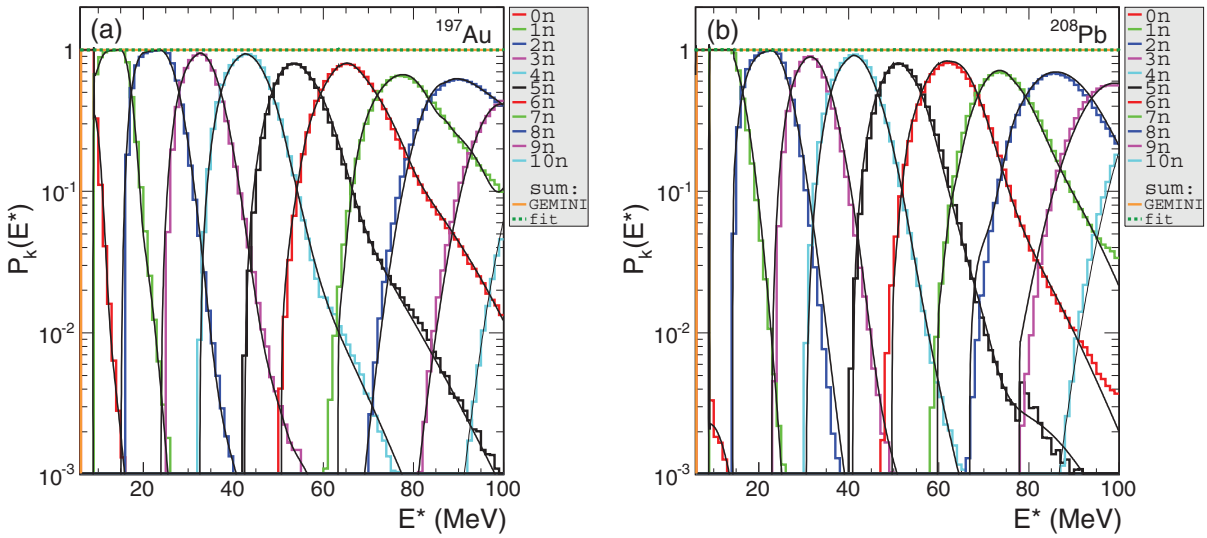

FIG. 6. (Color online) Probability of neutron multiplicity as a function of excitation energy (E^*) of ^{197}Au nuclei (left panel) and of ^{208}Pb nuclei (right panel).

TABLE I. Parameters of fit functions for the probability of neutron multiplicity $P_k(E^*)$ for the Pb nucleus.

Number of neutrons	C_e	μ_e	σ_e	C_G	μ_G	σ_G
0	0	–	–	0.02	9	3.5
1	0	–	–	9.9	12	3.5
2	0.08	21.6	1.7	10.3	21.5	4.2
3	0.0015	38	1.2	9.4	31.5	4.2
	0.0005	40	2.6			
4	0.0012	45	2.3	11	41	4.8
	0.000008	62	8			
5	0.03	53	2.6	8.7	51	4.3
	0.00015	72	4.9			
6	0.023	62.2	2.8	11.5	61.8	5.5
	0.003	68	4.35			
7	0.015	76	4	9.5	73.5	5.3
8	0	–	–	8.8	84	5.3
9	0	–	–	10.5	99	7.2
10	0	–	–	10.1	110	6.5

quality of the description of the data is fully sufficient for our purpose.

A. Decays of excited nuclear systems

The calculation of the probability of evaporated neutron multiplicity as a function of ^{197}Au and ^{208}Pb excitation energy was performed with the help of the Monte Carlo code GEMINI++ [15]. In this code the evaporation process is described by the Hauser-Feshbach formalism [16], in which the decay width for evaporation of a particle i from the compound nucleus with excitation energy E^* and spin S_{CN} is

$$\Gamma_i = \frac{1}{2\pi\rho(E^*,S_{CN})}\int d\epsilon \sum_{S_d=0}^{\infty}\sum_{J=|S_{CN}-S_d|}^{S_{CN}+S_d}\sum_{\ell=|J-S_i|}^{J+S_i} \times T_\ell(\epsilon)\rho(E^*-B_i-\epsilon,S_d), \quad (3.8)$$

where S_d is the spin of the daughter nucleus; S_i, J, and ℓ are the spin, total, and angular momentum of the evaporated particle; ϵ, B_i are the kinetic and separation energies; T_ℓ is its transmission coefficient; and ρ and ρ_{CN} are level densities of the daughter and compound nucleus, which can be calculated from the formula

$$\rho(E^*,S) \propto (2S+1)\exp(2\sqrt{a(U,S)U}), \quad (3.9)$$

where $U = E^* - E_{\rm rot}(S) - \delta P$ is the thermal excitation energy calculated by taking into account pairing corrections to the empirical mass formula (δP) and rotational energy $E_{\rm rot}(S)$. In the calculations the separation energies B_i, nuclear masses, shell, and pairing corrections were used as in Ref. [17]. The level density parameter $a(U,S)$ was calculated as

$$a(U,S) = \tilde{a}(U)\left(1 - h(U/\eta + S/S_\eta)\frac{\delta W}{U}\right), \quad (3.10)$$

where δW is the shell correction to the liquid-drop mass and $\tilde{a}$ is the smoothed level-density parameter, the function specifying the rate of fadeout is $h(x) = \tanh x$, the fadeout parameter η was equal to 18.52 MeV, and the parameter S_η was set to 50 $\hbar$.

The smoothed level density parametrization depends on the nuclei excitation energy as

$$\tilde{a}(U) = \frac{A}{k_\infty - (k_\infty - k_0)\exp\left(-\frac{\kappa}{k_\infty - k_0}\frac{U}{A}\right)}, \quad (3.11)$$

where $k_0 = 7.3$, $k_\infty = 12$, and $\kappa = 0.00517\exp(0.0345A)$ [15].

We assume that the excited nucleus is formed with angular momentum equal to 0 (which we believe is a good approximation for photoproduction) and the full energy is used for excitation. The calculation is done with an energy step of 1 MeV. For each excitation energy, 10^5 events (decays) were generated. Finally, neutron emissions probabilities were obtained from the Monte Carlo sample for each excitation energy (see the histograms in Fig. 6).

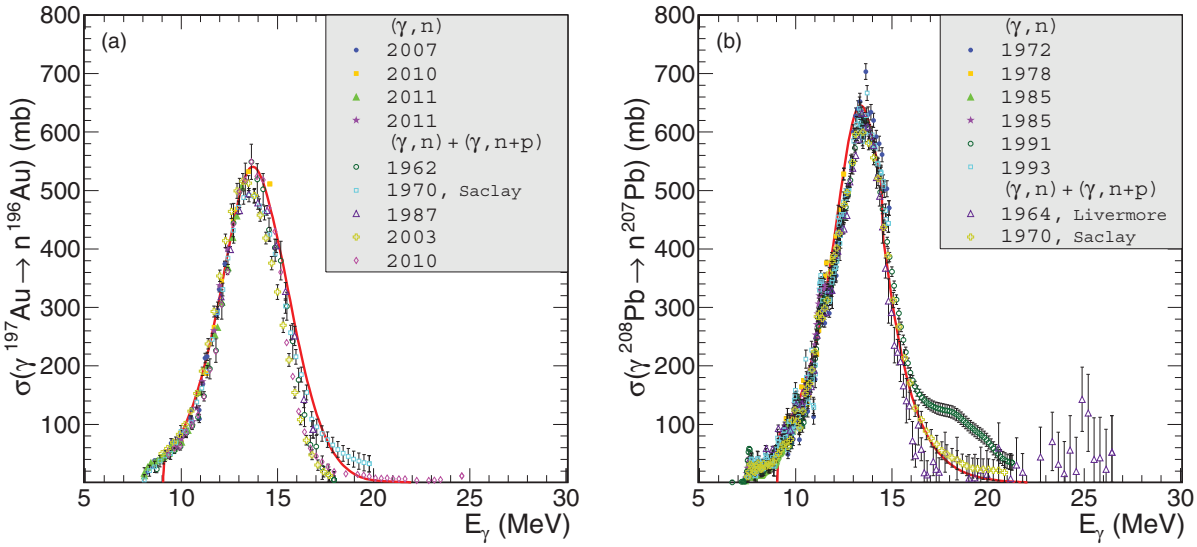

FIG. 7. (Color online) Excitation function for the $\gamma\,^{197}\mathrm{Au} \rightarrow \mathrm{n}^{196}\mathrm{Au}$ reaction (left panel; experimental data are from Refs. [10,11,18–25]) and for the $\gamma\,^{208}\mathrm{Pb} \rightarrow \mathrm{n}^{207}\mathrm{Pb}$ reaction (right panel; data are from Refs. [10,25–31]).

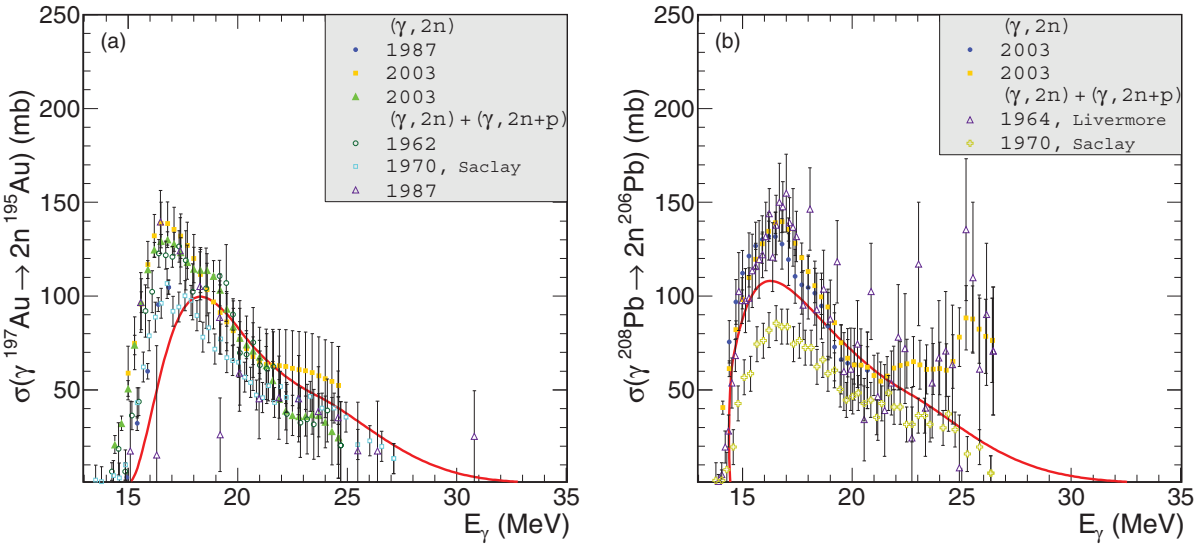

FIG. 8. (Color online) Excitation function for the $\gamma\,^{197}\mathrm{Au} \rightarrow 2\mathrm{n}^{195}\mathrm{Au}$ reaction (left panel; experimental data are from Refs. [10,22–24,32]) and for the $\gamma\,^{208}\mathrm{Pb} \rightarrow 2\mathrm{n}^{206}\mathrm{Pb}$ reaction (right panel; data are from Refs. [10,24,31]).

The fractions of events with a k-neutron final state at excitation energy E^* can be well fitted by a sum of the following purely empirical functions:

$$f(E^*,k) = f^{\mathrm{exp}}(E^*,k) + f^{\mathrm{Gauss}}(E^*,k). \tag{3.12}$$

$$f^{\mathrm{exp}}(E^*,k) = C_e(E^* - \mu_e)^2 \exp\left(\frac{-(E^* - \mu_e)}{\sigma_e}\right), \tag{3.13}$$

$$f^{\mathrm{Gauss}}(E^*,k) = \frac{C_G}{\sigma_G\sqrt{2\pi}} \exp\left(\frac{-(E^* - \mu_G)^2}{2\sigma_G^2}\right). \tag{3.14}$$

The parameters of the phenomenological functions found in the fit for Pb are collected in Table I and can be used in any calculations. For Au there are more parameters (more terms used in the parametrization). Those parameters can be obtained on request from the authors.

To ensure that probabilities always add up to unity, in practice we impose

$$\begin{aligned} f(E^*,2) &= 1 - f(E^*,1) \text{ for } E^* < 22\,\mathrm{MeV}, \\ f(E^*,3) &= 1 - f(E^*,1) - f(E^*,2) \text{ for } E^* < 30\,\mathrm{MeV}, \end{aligned} \tag{3.15}$$

and similarly for higher k.

B. Excitation functions for the γAu→Au* → kn and for the γPb→Pb* → kn reactions

Using the photoabsorption cross section shown in Fig. 5 and the probability to emit a fixed number k of neutrons obtained

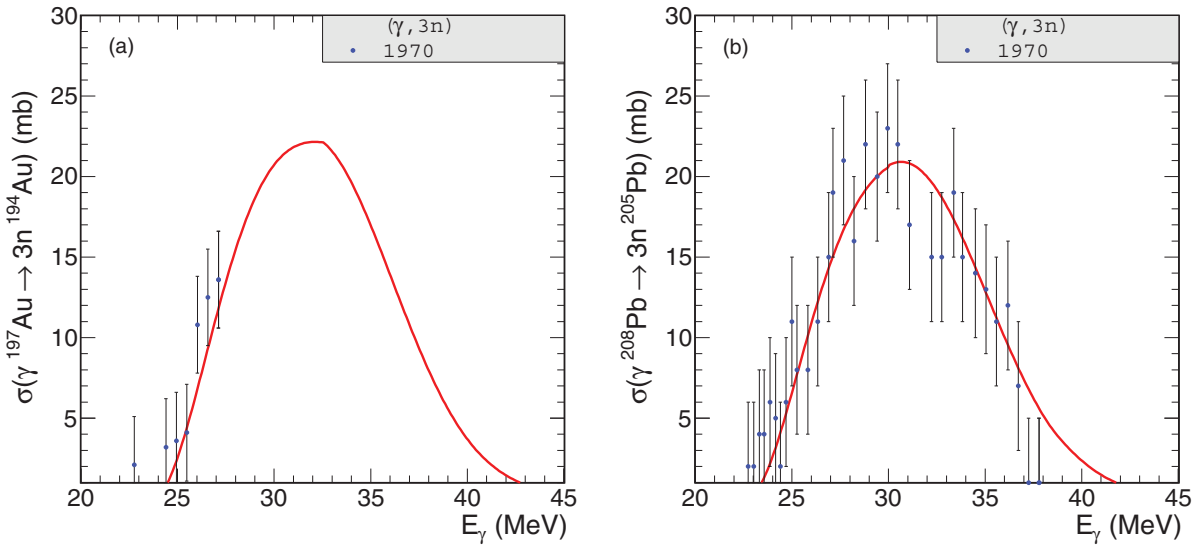

FIG. 9. (Color online) Excitation function for the $\gamma\,^{197}\mathrm{Au} \rightarrow 3\mathrm{n}^{194}\mathrm{Au}$ reaction (left panel; experimental data are from Ref. [10]) and for the $\gamma\,^{208}\mathrm{Pb} \rightarrow 3\mathrm{n}^{205}\mathrm{Pb}$ reaction (righ panel; data are from Ref. [10]).

TABLE II. Cross section in barns for single-nucleus, single-photon excitation for different ranges of excitation energy for ^{197}Au + ^{197}Au collisions; $\sqrt{s_{NN}} = 200$ GeV.

	$\sigma_{\rm dis}$		
	Our results		
$\omega_{\rm max}$ (MeV)	with exp($-\bar{n}$)	without exp($-\bar{n}$)	Baltz *et al.* [33]
25	65.0	66.7	65
103	71.4	73.5	70
440	82.7	84.9	82
2000	89.9	92.2	90
17840	94.0	96.4	94

as described in Sec. III, we can calculate the photon-induced excitation function with a given number of associated neutrons. The results are shown in Figs. 7, 8, and 9.

Quite a good agreement with the world data is obtained. This is quite surprising given that our calculation implicitly assumes equilibration of the nuclear system (Hauser-Feshbach formalism) formed after the absorption of the photon. If we assumed that part of the energy of the photon would escape before equilibration of the nuclear system (due to pre-equilibrium processes) the agreement with the data would be much worse. Having proven the usefulness of our approach, we can proceed to the excitation of nuclei in UPCs and the related production of neutrons from the excited nuclear systems. In the following we shall present the results of the formalism discussed above.

IV. RESULTS FOR ELECTROMAGNETIC EXCITATIONS IN UPCS

Now we shall present our results for electromagnetic excitation of nuclei in UPCs.

In Table II we show the dissociation cross section at the RHIC energy. We compare the cross section obtained by us to the numbers given in Ref. [33]. Our results, which include exponential factors [see Eq. (2.17)] extremely well, agree with those obtained by Baltz *et al.* The effect of including exponential factors is, however, rather small (about 2%).

TABLE III. Cross section in barns for single-nucleus, single-photon excitation for different ranges of excitation energy for ^{208}Pb + ^{208}Pb collisions.

	(6–40) MeV	(40–2000) MeV	(2–80) GeV
	$\gamma_{\rm c.m.} = 100$		
Vidović *et al.* [13]	77.6	25.7	5.6
Our results with exp($-\bar{n}$)	77.7	26.1	5.6
without exp($-\bar{n}$)	80.2	27.4	5.6
	$\gamma_{\rm c.m.} = 3100$		
Vidović *et al.* [13]	133.6	53.7	18.7
Our results with exp($-\bar{n}$)	133.4	55.1	18.8
without exp($-\bar{n}$)	135.0	55.8	18.9

TABLE IV. Cross section in barns [with and without extra exponential (exp($-\bar{n}$)) factor] for a given multiplicity of neutrons in single-nucleus, single-photon excitation in ^{197}Au + ^{197}Au collisions at $\sqrt{s_{NN}} = 130$ GeV.

	Our results	
	with exp($-\bar{n}$)	without exp($-\bar{n}$)
0 neutrons	5.613	5.919
1 neutron	45.076	47.133
2 neutrons	8.456	8.862
3 neutrons	1.551	1.629
4 neutrons	1.049	1.105
5 neutrons	0.707	0.746
6 neutrons	0.655	0.691
$\sum_{k=1}^{k=6}$	57.494	60.691
total ($\sum_{k>0}$)	79.989	84.637

In Table III we collect the cross section in barns for one-nucleus single-photon excitation for different ranges of the excitation energy and the different collision energies represented by different $\gamma_{\rm c.m.}$ adequate for RHIC and LHC. The calculation was done for Pb nuclei even at lower (RHIC) energy to compare to the results published in Ref. [13]. Our results are compared to the earlier calculation by Vidović *et al.* [13]. Very good agreement can be observed when the exponential factors are included.

As already discussed, we are very interested also in calculating the associated neutron multiplicities. In Table IV we show the cross section for neutron emission from only one Au nucleus relevant for the RHIC energy $\sqrt{s_{NN}} = 130$ GeV. The effect of the inclusion of the exponential factor leads to fairly uniform damping of the cross section.

In Table V we have collected similar cross sections as in the previous case (one-photon single-nucleus excitation in barns for different neutron multiplicities $k = 0,1,2,3,4,5,6$), but for the Pb-Pb collisions at $\sqrt{s_{NN}} = 2.76$ TeV. Again we compare results with and without the exponential factor. As can be seen from the table, the exponential factor plays here only a minor role in practical calculations for single-nucleus

TABLE V. Cross section (in barns) for a given multiplicity of neutrons in single-nucleus, single-photon excitation in ^{208}Pb + ^{208}Pb collisions at $\sqrt{s_{NN}} = 2.76$ TeV.

	Our results		
	with exp($-\bar{n}$)	without exp($-\bar{n}$)	ALICE (Ref. [34])
0 neutrons	5.524	5.815	
1 neutron	89.181	93.768	93.37 ± 6.90
2 neutrons	19.262	20.065	21.03 ± 2.43
3 neutrons	2.933	3.024	6.53 ± 0.94
4 neutrons	1.995	2.059	
5 neutrons	1.356	1.427	
6 neutrons	1.334	1.404	
$\sum_{k=1}^{k=6}$	116.660	121.748	
total ($\sum_{k>0}$)	173.776	179.765	$187.4\ ^{+13.2}_{-11.2}$

TABLE VI. Summary of cross sections (in barns) for $\sqrt{s_{NN}} = 130$ GeV.

$\sqrt{s_{NN}} = 130$ GeV		$\sigma(1,X)$	$\sigma(1,1)$	$\sigma(2,X)$
PHENIX [35]		1.264 ± 0.102	0.434 ± 0.042	0.436 ± 0.053
PHOBOS [35]		1.328 ± 0.119	0.454 ± 0.053	0.448 ± 0.060
BRAHMS [35]		1.307 ± 0.158	0.475 ± 0.065	0.457 ± 0.094
Baltz *et al.* [36]		1.350	0.443 ± 0.042	–
Pshenichnov *et al.* [37]		1.557	–	0.509
Our results	with $\exp(-\bar{n})$	1.133	0.5082	0.223
	without $\exp(-\bar{n})$	2.593	1.1541	0.511

excitation. We have also collected the experimental data of the ALICE collaboration [34]. We observe some disagreement especially for three neutrons. For the ratio $2n/1n$ we obtain 21.6% (with an extra exponential factor) or 21.4% [without $\exp(-\bar{n})$], in good agreement with the ALICE result of 22.5 ± 0.5 stat ± 0.9 syst %.

In Table VI we refer to the data published in Ref. [35], where the ratios $\sigma(1,X)/\sigma_{\rm tot}$, $\sigma(1,1)/\sigma_{\rm tot}$, and $\sigma(2,X)/\sigma(1,X)$ were collected. In our table we have collected also the corresponding values by Baltz *et al.* [36] and Pschenichnov *et al.* [37]. To obtain our cross sections in barns we multiplied the ratios given in Ref. [35] by the $\sigma_{\rm tot} = 10.8$ b taken from the same reference. We have fairly good agreement with the experimental data for one-neutron emissions and rather bad agreement for two-neutron emissions.

Two-photon exchanges may also lead to the simultaneous excitation of both nuclei (see Fig. 3). In Tables VII and VIII we collected topological cross sections with a given number of neutrons emitted from the first (k_1) and second (k_2) nuclei. As previously, we show the results of the calculation with and without the extra exponential factor, which seems here more important than for one-nucleus single-photon excitations. For example, for the $(1n,1n)$ emission the effect of the exponential factor decreases the cross section by about 44% for RHIC and LHC. This indicates the importance of smaller impact parameters in the mutual neutron emissions compared to single-nucleus emissions. Our results can be compared to those in Ref. [6]. Compared to Ref. [6] our cross section for neutron multiplicities $k_1 = 1$ and $k_2 = 1$ are smaller by 17% for RHIC and 5% for LHC energies. Other numbers seem to be in much better agreement. The differences quantify the uncertainties of the theoretical calculations.

The emission of a few neutrons corresponds to relatively low excitations of nuclei ($E^* < 100$ MeV). The total cross sections for mutual excitations can be expected to be much larger. In Tables IX and X we show the contribution to mutual excitations from different regions of excitation energy of the first and second nuclei for RHIC and LHC, respectively. $E_{\rm min} = 8$ MeV corresponds to the neutron binding energy. The situation when each of the nuclei is excited below 100 MeV constitutes only around one-third. Quite large ranges of excitation energies ($E_1^*, E_2^* > 10$ GeV) contribute to the mutual excitation. The sum of the cross sections corresponding to the different regions adequately describe the experimentally

TABLE VII. Mutual cross section (in barns) with a given number of neutrons emitted from both nuclei in ^{197}Au + ^{197}Au collisions at the RHIC energy $\sqrt{s_{NN}} = 130$ GeV.

	$1n$	$2n$	$3n$	$4n$	$5n$	$6n$	$\exp(-\bar{n})$
$1n$	0.5082	0.1002	0.0195	0.0137	0.0096	0.0091	with
	1.1541	0.2276	0.0442	0.0311	0.0217	0.0207	without
$2n$	0.1002	0.0198	0.0038	0.0027	0.0019	0.0018	with
	0.2276	0.0449	0.0087	0.0061	0.0043	0.0041	without
$3n$	0.0195	0.0038	0.0007	0.0005	0.0004	0.0003	with
	0.0442	0.0087	0.0017	0.0012	0.0008	0.0008	without
$4n$	0.0137	0.0027	0.0005	0.0004	0.0003	0.0002	with
	0.0311	0.0061	0.0012	0.0008	0.0006	0.0006	without
$5n$	0.0096	0.0019	0.0004	0.0003	0.0002	0.0002	with
	0.0217	0.0043	0.0008	0.0006	0.0004	0.0004	without
$6n$	0.0091	0.0018	0.0003	0.0002	0.0002	0.0002	with
	0.0207	0.0041	0.0008	0.0006	0.0004	0.0004	without
$\sum$	0.6603	0.1302	0.0252	0.0178	0.0126	0.0118	with
	1.4994	0.2957	0.0574	0.0404	0.0282	0.0270	without
$\sum$			0.8579				with
			1.9211				without

TABLE VIII. Cross section in barns for mutual excitation with a given number of neutrons emitted from both nuclei in ^{208}Pb + ^{208}Pb collisions at $\sqrt{s_{NN}} = 2.76$ TeV.

	$1n$	$2n$	$3n$	$4n$	$5n$	$6n$	$\exp(-\bar{n})$
$1n$	0.7043	0.1543	0.0248	0.0168	0.0121	0.0116	with
	1.6008	0.3502	0.0546	0.0379	0.0271	0.0263	without
$2n$	0.1543	0.0339	0.0052	0.0037	0.0026	0.0025	with
	0.3502	0.0766	0.0119	0.0083	0.0059	0.0058	without
$3n$	0.0248	0.0052	0.0009	0.0006	0.0004	0.0004	with
	0.0546	0.0119	0.0019	0.0013	0.0009	0.0009	without
$4n$	0.0168	0.0037	0.0006	0.0004	0.0003	0.0003	with
	0.0379	0.0083	0.0013	0.0009	0.0006	0.0006	without
$5n$	0.0121	0.0026	0.0004	0.0003	0.0002	0.0002	with
	0.0271	0.0059	0.0009	0.0006	0.0005	0.0004	without
$6n$	0.0116	0.0025	0.0004	0.0003	0.0002	0.0002	with
	0.0263	0.0058	0.0009	0.0006	0.0004	0.0004	without
$\sum$	0.9239	0.2022	0.0323	0.0221	0.0158	0.0152	with
	2.0915	0.4587	0.0715	0.0496	0.0354	0.0344	without
$\sum$			1.2115				with
			2.7411				without

TABLE IX. Mutual cross section (in barns) for RHIC. Shown are contributions from different regions of excitation energies of the first and second nuclei.

$\sqrt{s_{NN}} = 130$ GeV	$E_1 = (8–100)$ MeV	$E_1 = (100–1000)$ MeV	$E_1 = (1–10)$ GeV	$E_1 = (10–100)$ GeV	$\exp(-\bar{n})$
$E_2 = (8–100)$ MeV	1.3075	0.5142	0.3018	0.1444	with
	2.2520	0.7485	0.4242	0.2053	without
$E_2 = (100–1000)$ MeV	0.5142	0.2049	0.1208	0.0592	with
	0.7485	0.2488	0.1410	0.0683	without
$E_2 = (1–10)$ GeV	0.3018	0.1208	0.0714	0.0353	with
	0.4242	0.1410	0.0800	0.0389	without
$E_2 = (10–100)$ GeV	0.1444	0.0592	0.0353	0.0182	with
	0.2053	0.0683	0.0389	0.0196	without
$\sum$	2.2679	0.8994	0.5293	0.2571	with
	3.6300	1.2066	0.6841	0.3321	without
$\sum$		3.9537			with
		5.8528			without
RHIC Ref. [35]		3.67 ± 0.26			

measured cross section at RHIC and LHC as shown at the bottom of each table.

Excitation functions are particularly interesting. In Fig. 10 we show the total cross section for electromagnetic excitation as a function of $\sqrt{s_{NN}}$ as well as the partial cross sections into one-neutron and two-neutron final states. We get very good agreement with the experimental data for both Super Proton Synchrotron (SPS) and LHC. It should be noted that we concentrate only on the neutrons evaporated from the electromagnetically excited nuclei. We do not account for neutrons from other hadronic processes, like the intranuclear cascading (see, for example, Refs. [6,37]). We also neglect the mutual excitation of nuclei by strong interactions.

In Fig. 11 we show our result for the $^{197}\mathrm{Au} + {}^{197}\mathrm{Au} \to {}^{197}\mathrm{Au}^* + {}^{197}\mathrm{Au}$ reaction at the RHIC energy $\sqrt{s_{NN}} = 130$ GeV and for $^{208}\mathrm{Pb} + {}^{208}\mathrm{Pb} \to {}^{208}\mathrm{Pb}^* + {}^{208}\mathrm{Pb}$ reaction at the LHC energy $\sqrt{s_{NN}} = 2.76$ TeV. For technical reasons different regions [low (6–40 MeV), intermediate (40–2000 MeV), and high (>2 GeV)] of excitation energy were calculated separately. The dashed line represents the contribution of single-photon excitation (diagram in Fig. 1) and the dotted line double-photon excitation (diagram in Fig. 2). Both leading-order and next-to-leading order contributions reflect the maxima present in the spectrum of the photoexcitation of Au or Pb nuclei. The double-photon contribution is rather small. Even at the very high collision energy the low-energy excitations are still essential. Please note, however, the logarithmic scale for the excitation energy axis, which emphasises the low-energy excitation. The double-photon excitation contribution is much smaller than the single-photon one. In addition, the highest peak appears at the excitation energy two times larger than for single-photon excitation, which corresponds to the excitation of the giant dipole resonance excited on top of an already excited one. Such processes were already discussed in the literature (see Ref. [6] and the references therein).

V. CONCLUSION

In this paper we present a new approach for calculating the excitation of Au and Pb nuclei in photoabsorption reactions as

TABLE X. Mutual cross section (in barns) for LHC. Shown are contributions from different regions of excitation energies of the first and second nuclei.

$\sqrt{s_{NN}} = 2.76$ TeV	$E_1 = (8–100)$ MeV	$E_1 = (100–1000)$ MeV	$E_1 = (1–10)$ GeV	$E_1 = (10–100)$ GeV	$\exp(-\bar{n})$
$E_2 = (8–100)$ MeV	1.6252	0.7289	0.3847	0.2661	with
	3.0173	1.1346	0.5661	0.3845	without
$E_2 = (100–1000)$ MeV	0.7289	0.3319	0.1760	0.1219	with
	1.1346	0.4267	0.2129	0.1446	without
$E_2 = (1–10)$ GeV	0.3847	0.1760	0.0934	0.0648	with
	0.5661	0.2129	0.1062	0.0721	without
$E_2 = (10–100)$ GeV	0.2661	0.1219	0.0648	0.0203	with
	0.3845	0.1446	0.0721	0.0219	without
$\sum$	3.0049	1.3587	0.7189	0.4731	with
	5.1025	1.9188	0.9573	0.6231	without
$\sum$		5.5556			with
		8.6017			without
ALICE, Ref. [34]		$5.7 \pm 0.1(\mathrm{stat}) \pm 0.4(\mathrm{syst}) = 5.7 \pm 0.412$			

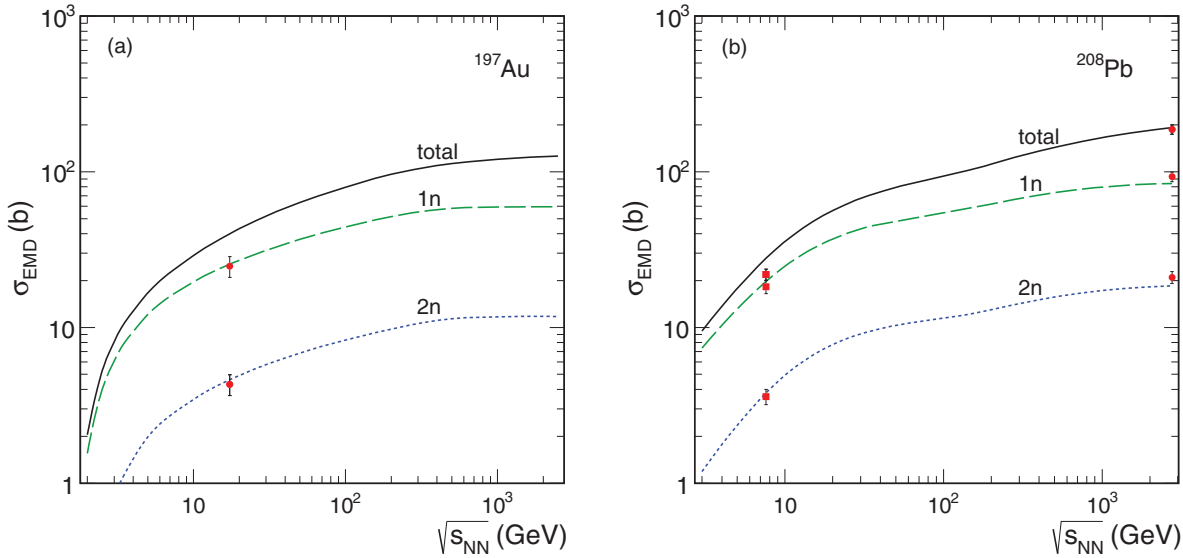

FIG. 10. (Color online) Single Electromagnetic Dissociation (EMD) cross sections as the function of $\sqrt{s_{NN}}$. Left panel depicts the results for Au nuclei (data are taken from SPS Ref. [38]; Au-Pb collision data rescaled to Au-Au case) and right panel shows the results for Pb nuclei (data are from SPS [39] and LHC (ALICE) [34]).

well as in ultraperipheral, ultrarelativistic heavy ion collisions. The photoabsorption cross section on Au and Pb nuclei are fitted using physics-motivated multicomponent parametrization. The giant resonances, quasideuteron, excitation of nucleon resonances, and breakup of the nucleon mechanism are included in the fit to the world data.

The neutron emission from the excited nuclear system is calculated within the Hauser-Feshbach formalism. Within our approach we get a very good description of the excitation functions for $\gamma + {}^{197}$Au and $\gamma + {}^{208}$Pb with a fixed number of neutrons. The excitation function is used next to calculate the cross sections in UPCs. Both single-photon and double-photon excitation processes are included and discussed. We calculated the corresponding excitation functions for single excitations.

We obtain a good agreement of the calculated total cross section for electromagnetic excitation as well as the cross section for one-neutron and two-neutron emissions with the recent experimental data of PHENIX, PHOBOS, BRAHMS, and ALICE collaborations.

The formalism presented here may be easily applied to other exclusive ultrarelativistic heavy ion processes such as $AA \to AAJ/\Psi$, $AA \to AA\rho^0$, $AA \to AAe^+e^-$, $AA \to AA\mu^+\mu^-$,

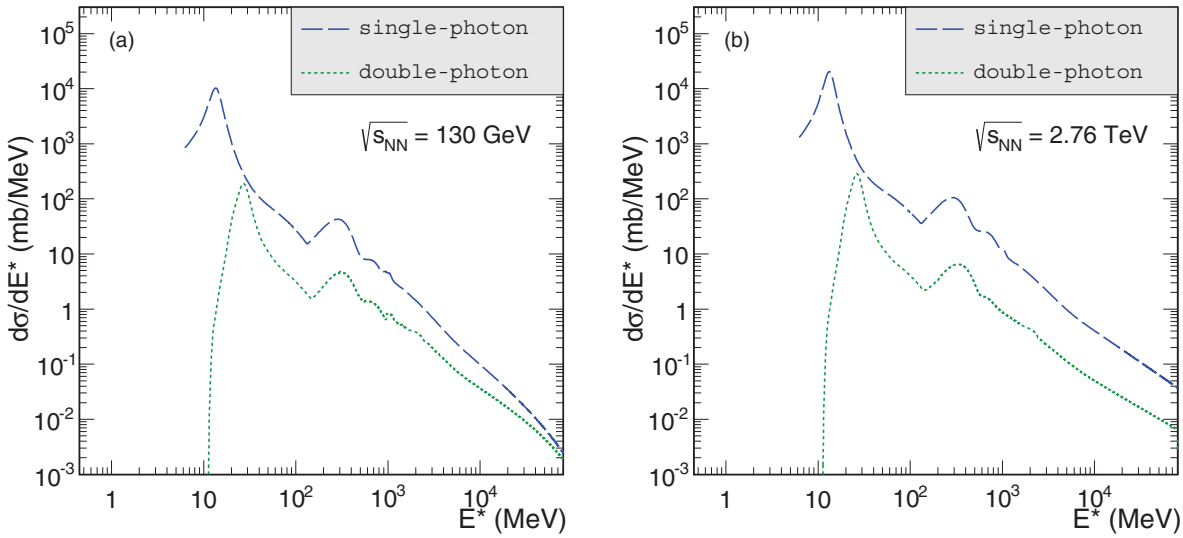

FIG. 11. (Color online) Excitation function $\frac{d\sigma}{dE^*}$ for electromagnetic excitation of one nucleus in single-photon (dashed) and double-photon (dotted) exchanges in UPCs at $\sqrt{s_{NN}} = 130$ GeV (left panel) and $\sqrt{s_{NN}} = 2.76$ TeV (right panel).

$AA \to AA\pi^+\pi^-$, and $AA \to AA\pi^+\pi^-\pi^+\pi^-$. This will be discussed in our future analyses.

ACKNOWLEDGMENTS

We would like to thank Igor Pshenichnov for the correspondence and Christoph Mayer and Joakim Nystrand for discussions. This work was partially supported by the Polish Grants No. N202 236640 and DEC-2011/01/B/ST2/04535 as well as by the Centre for Innovation and Transfer of Natural Sciences and Engineering Knowledge in Rzeszów. M.K. is grateful for financial support for the preparation of the doctoral dissertation from the National Science Centre in the framework of a doctoral scholarship financing based on the decision number 2013/08/T/ST/00669. A part of the calculations within this analysis was carried out with the help of a cloud computer system (Cracow Cloud One[1]) of the Institute of Nuclear Physics (PAN).

[1] cc1.ifj.edu.pl

[1] V. M. Budnev, I. F. Ginzburg, G. V. Meledin, and V. G. Serbo, Phys. Rep. **15**, 181 (1975); C. A. Bertulani and G. Baur, *ibid.* **163**, 299 (1988); G. Baur, K. Hencken, D. Trautmann, S. Sadovsky, and Y. Kharlov, *ibid.* **364**, 359 (2002); C. A. Bertulani, S. R. Klein, and J. Nystrand, Ann. Rev. Nucl. Part. Sci. **55**, 271 (2005); A. J. Baltz *et al.*, Phys. Rep. **458**, 1 (2008).

[2] M. Kłusek, A. Szczurek, and W. Schäfer, Phys. Lett. B **674**, 92 (2009); M. Kłusek-Gawenda and A. Szczurek, Phys. Rev. C **82**, 014904 (2010); M. Kłusek-Gawenda, A. Szczurek, M. V. T. Machado, and V. G. Serbo, *ibid.* **83**, 024903 (2011); S. Baranov, A. Cisek, M. Kłusek-Gawenda, W. Schäfer, and A. Szczurek, Eur. Phys. J. C **73**, 2335 (2013); M. Kłusek-Gawenda and A. Szczurek, Phys. Lett. B **700**, 322 (2011); Phys. Rev. C **87**, 054908 (2013); arXiv:1309.2463.

[3] C. Adler, A. Denisov, E. Garcia, M. Murray, H. Stroebele, and S. White, Nucl. Instrum. Meth. **A470**, 488 (2001).

[4] K. Aamodt *et al.* (ALICE Collaboration), J. Instrum. **3**, S08002 (2008).

[5] W. J. Llope and P. Braun-Munzinger, Phys. Rev. C **41**, 2644 (1990).

[6] I. A. Pshenichnov, Phys. Part. Nucl. **42**, 215 (2011).

[7] G. Baur, K. Hencken, A. Aste, D. Trautmann, and S. R. Klein, Nucl. Phys. A **729**, 787 (2003).

[8] V. A. Plujko, R. Capote, and O. M. Gorbachenko, At. Data Nucl. Data Tables **97**, 567 (2011).

[9] J. Speth and A. van der Woude, Rep. Progr. Phys. **44**, 719 (1981).

[10] A. Veyssiere, H. Beil, R. Bergere, P. Carlos, and A. Lepretre, Nucl. Phys. A **159**, 561 (1970).

[11] V. V. Varlamov, M. E. Stepanov, and V. V. Chesnokov, Izv. Ross. Akad. Nauk, Ser. Fiz. **67**, 656 (2003).

[12] M. B. Chadwick, P. Oblozinsky, P. E. Hodgson, and G. Reffo, Phys. Rev. C **44**, 814 (1991).

[13] M. Vidović, M. Greiner, and G. Soff, Phys. Rev. C **48**, 2011 (1993).

[14] J. Ahrens, Nucl. Phys. A **446**, 229 (1985).

[15] R. J. Charity, Phys. Rev. C **82**, 014610 (2010).

[16] W. Hauser and H. Feshbach, Phys. Rev. **87**, 366 (1952).

[17] P. Möller, J. R. Nix, W. D. Myers, and W. J. Swiatecki, At. Data Nucl. Data Tables **59**, 185 (1995).

[18] K. Y. Hara, H. Harada, F. Kitatani, S.Goko, S. Hohara, T. Kaihori, A. Makinaga, H. Utsunomiya, H. Toyokawa, and K. Yamada, J. Nucl. Sci. Technol. **44**, 938 (2007).

[19] F. Kitatani, H. Harada, S. Goko, H. Utsunomiya, H. Akimune, T. Kaihori, H. Toyokawa, and K. Yamada, J. Nucl. Sci. Technol. **47**, 367 (2010).

[20] O. Itoh, H. Utsunomiya, H. Akimune, T. Kondo, M. Kamata, T. Yamagata, H. Toyokawa, H. Harada, F. Kitatani, S. Goko, C. Nair, and Y.-W. Lui, J. Nucl. Sci. Technol. **48**, 834 (2011).

[21] F. Kitatani, H. Harada, S. Goko, H. Utsunomiya, H. Akimune, H. Toyokawa, and K. Yamada, J. Nucl. Sci. Technol. **48**, 1017 (2011).

[22] S. C. Fultz, R. L. Bramblett, J. T. Caldwell, and N. A. Kerr, Phys. Rev. **127**, 1273 (1962).

[23] B. L. Berman, R. E. Pywell, S. S. Dietrich, M. N. Thompson, K. G. McNeill, and J. W. Jury, Phys. Rev. C **36**, 1286 (1987).

[24] V. V. Varlamov, N. N. Peskov, D. S. Rudenko, and M. E. Stepanov, Yadernye Konstanty (Nuclear Constants) (in Russian) **1–2**, 48 (2003).

[25] V. V. Varlamov, N. G. Efimkin, B. S. Ishkhanov, and V. V. Sapunenko, Nuclear Constants **1**, 52 (1993).

[26] L. M. Young, PhD. thesis, University of Illinois at Urbana-Champaign, 1972.

[27] R. Van de Vyver, J. Devos, H. Ferdinande, R. Carchon, and E. Van Camp, Z. Phys. A **284**, 91 (1978).

[28] S. N. Belyaev, A. B. Kozin, A. A. Nechkin, V. A. Semenov, and S. F. Semenko, Yad. Fiz. **42**, 1050 (1985).

[29] S. N. Belyaev, O. V. Vasilev, A. B. Kozin, A. A. Nechkin, and V. A. Semenov, Program and Theses, in Proceedings of the 35th Ann. Conf. Nucl. Spectrosc. Struct. At. Nuclei, Leningrad (1985), p. 351.

[30] S. N. Belyaev, A. A. Nechkin, and V. A. Semenov, Izv. Ross. Akad. Nauk, Ser. Fiz. **55**, 953 (1991).

[31] R. R. Harvey, J. T. Caldwell, R. L. Bramblett, and S. C. Fultz, Phys. Rev. **136**, B126 (1964).

[32] V. V. Varlamov, B. S. Ishkhanov, V. N. Orlin, and S. Yu. Troshchiev, Izv. Ross. Akad. Nauk, Ser. Fiz. **74**, 884 (2010).

[33] A. J. Baltz, M. J. Rhoades-Brown, and J. Weneser, Phys. Rev. E **54**, 4233 (1996).

[34] B. Abelev *et al.* (ALICE Collaboration), Phys. Rev. Lett. **109**, 252302 (2012).

[35] M. Chiu, A. Denisov, E. Garcia, J. Katzy, A. Makeev, M. Murray, and S. White, Phys. Rev. Lett. **89**, 012302 (2002).

[36] A. J. Baltz, C. Chasman, and S. N. White, Nucl. Instrum. Meth. A **417**, 1 (1998).

[37] I. A. Pshenichnov, J. P. Bondorf, I. N. Mishustin, A. Ventura, and S. Masetti, Phys. Rev. C **64**, 024903 (2001).

[38] J. C. Hill, A. Petridis, B. Fadem, and F. K. Wohn, Nucl. Phys. A **661**, 313 (1999).

[39] M. B. Golubeva *et al.*, Phys. Rev. C **71**, 024905 (2005).